Plant Physiol. (1986) 80, 752–759
0032-0889/86/80/0752/08/$01.00/0

Diurnal Changes in Volume and Solute Transport Coefficients of *Phaseolus* Roots

Received for publication August 1, 1985 and in revised form November 12, 1985

EDWIN L. FISCUS
United States Department of Agriculture, Agricultural Research Service, Crops Research Laboratory, Colorado State University, Fort Collins, Colorado 80523

ABSTRACT

Volume (J_v) and solute (J_s) fluxes through *Phaseolus* root systems were observed over a 24-hour period. The volume flux was varied in a pressure chamber by altering the hydrostatic pressure in 10 steps, from 0 to 0.41 megapascals. All root systems showed strong diurnal peaks in volume flux. The five transport coefficients (σ, ω, J_s^*, L_p, and π^*) were estimated from a nonlinear least squares algorithm. Analysis of the data revealed that all the coefficients exhibited a diurnal rhythm. When the total differential of the volume flux was considered it was possible to show that the diurnal changes in volume flux were due to a complex interaction between the diurnally shifting coefficients with the role of each highly dependent on the level of volume flux. At low volume fluxes, ω, J_s^*, and π^* accounted for nearly all the diurnal change in volume flux. At high volume fluxes, however, the major influence shifted to L_p and π^*, while ω and J_s^* became relatively unimportant. Thus, π^* was the only coefficient of interest across the entire range of J_v and appeared to be the single most important one in determining the diurnal rhythm of J_v under conditions of a constant applied pressure.

Since the first report of Hofmeister in 1862 (see Vaadia [27]) of the diurnal fluctuations of both root pressure and exudation rates, the phenomenon has been repeatedly demonstrated (more recently [11–13, 18, 21, 24, 27 29]) and investigated from several points of view. Recent studies have demonstrated that there is a diurnal periodicity of translocation of solutes to the shoot (14, 26, 28), but more significant perhaps are the observations of Wallace *et al.* (28) that there appears to be a difference in the time when some salts are absorbed and the time when they are transported to the shoot. Diurnal fluctuations in root conductance (alternatively resistance) to water flow have also been demonstrated (2, 21, 23). However, we have shown (4–6, 9) that changes in solute transport can manifest themselves as conductance changes when, in fact, the root hydraulic conductance coefficient may not change at all. In most of the above studies where conditions were adequately controlled, it was possible to demonstrate that the periodicity was endogenous but could be controlled, altered, or made to disappear by proper manipulation of the day-night cycle.

In none of the studies mentioned was a more specific analysis in terms of volume and solute transport coefficients possible. The purpose of this paper is then to analyze the diurnal rhythms of volume and solute transport in terms of flow models that include diffusive, convective, and active transport of solutes as well as the osmotic and hydrostatic forces that drive volume flux. Specifically, we want to discover which of the relevant transport coefficients, or combination thereof, might account for the often observed diurnal changes in volume and solute fluxes. We will demonstrate that the causes of the diurnal rhythms in solute and volume fluxes involve some fairly complex interactions among the various transport coefficients and their own diurnal to rhythms. We will further show that the contribution of each of the coefficients is highly dependent on the volume flux.

MATERIALS AND METHODS

Bean seeds (*Phaseolus vulgaris* [L] cv Ouray) were germinated in vermiculite for 4 d, then transferred to individual stainless steel pots filled with aerated half-strength Hoagland solution and grown in a greenhouse. Supplemental lighting gave a mean photosynthetic photon flux density of 270 μmol m^{-2} s^{-1} over a 14 h photoperiod (0600–2000) at the top of the plants. The plants, selected for size at the time of the experiments, averaged about 2230 cm^2 projected leaf area as measured with a LI-COR[1] model 3100 leaf area meter, and about 3150 cm^2 root surface area. Each root system was decapitated and sealed into a pressure chamber with the cut stump protruding through the lid and the roots surrounded by aerated nutrient solution (π^0 = 35 kPa)[2] as previously described (5). The plants were placed in the chamber at about 1600 h, brought to the specified pressure and temperature (25 ± 0.25°C), and allowed to equilibrate. Beginning at midnight, measurements of volume flow and ion flow from the cut stump were started and continued at 10-min intervals for the next 24 h. The volume flow was measured by weighing the exudate on an electronic balance. Concentration of the exudate was estimated from the electrical conductivity and expressed as KCl equivalents. The ion flow was then calculated as the product of the volume flow and the concentration. Using Newman's technique (19) on each root size class, surface areas were measured as described earlier (7) and the volume and ion fluxes calculated on a root area basis.

Ten separate plants were used, each subjected to a different applied pressure ranging from 0 to 0.41 MPa. The pressure on each root system was held constant for the duration of the experiment. Data for each root system were averaged for each hourly interval giving 24 data points (one for each hour) for each root system. After all 10 plants had been measured 24 separate volume flux-applied pressure ($J_v - \Delta P$) curves and 24 separate solute flux-volume flux ($J_s - J_v$) curves were constructed, one for each of the 24 h.

[1] Mention of specific product names does not constitute an endorsement by the United States Department of Agriculture.

[2] Abbreviations: π, osmotic pressure in Pa; P, hydrostatic pressure in Pa; J_s, solute flux mol m^{-2} s^{-1}; J_v, volume flux m^3 m^{-2} s^{-1}; C, concentration in mol m^{-3}; σ, tissue reflection coefficient (dimensionless); ω, diffusional solute mobility coefficient mol m^{-2} s^{-1} Pa^{-1}; R, universal gas constant J mol^{-1} K^{-1}; L_p, hydraulic conductance coefficient in m^3 m^{-2} s^{-1} Pa^{-1}; L_D, differential conductance in m^3 m^{-2} s^{-1} Pa^{-1}.

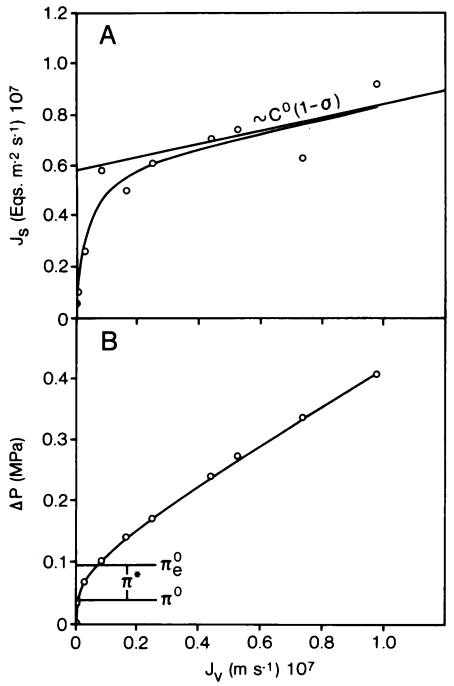

FIG. 1. The 24-h averages for J_v and J_s (circles in both A and B). The lines are calculated using coefficients in Table I. Note that π_e^0, obtained either by extrapolation of the linear portion of the curve back to the ordinate or by curve fitting, is the sum of π^0 (35 kPa) and π^*. (A) r^2 = 0.867; (B) r^2 = 0.992.

TRANSPORT EQUATIONS

The solute flux equation used was that given earlier by Fiscus (5) which includes the convective, diffusive, and active components of solute transport.

$$J_s = C^0 (1 - \sigma)J_v + \omega(\pi^0 - \pi^i) + J_s^*, \quad (1)$$

where C^0 is the medium concentration in mole m^{-3}, σ is the reflection coefficient, ω is the coefficient of solute mobility in mole m^{-2} s^{-1} MPa^{-1}, π^0 and π^i are the medium and xylem osmotic pressures, respectively, in MPa, J_s^* is the active solute transport in mole m^{-2} s^{-1} and J_v is the volume flux in m^3 m^{-2} s^{-1}. π^i is also an inverse function of J_v ($\pi^i = RTJ_s/J_v$) and Equation 1 must be expanded to account for this with the result that

$$J_s = \frac{C^0(1 - \sigma)J_v^2 + \omega\pi^0 J_v + J_s^* J_v}{J_v + \omega RT}. \quad (2)$$

At high J_v, the denominator in Equation 2 numerically approaches J_v and Equation 2 simplifies to

$$J_s \cong C^0(1 - \sigma)J_v + \omega\pi^0 + J_s^*, \quad (3)$$

which is linear in J_v with slope $C^0(1 - \sigma)$ (Fig. 1A). This fact is relevant to the fitting procedure and more will be said about it later.

The usual volume flux equation has been modified to account for the effects of an intermediate solute compartment between the exterior of the root and the xylem (5). The effect of this intermediate compartment is to shift the position of the $J_v - \Delta P$ curve with respect to the ordinate (Fig. 1B). Newman (20) noted that at high volume fluxes the $J_v - \Delta P$ curve approaches a straight line which when extrapolated back to the ordinate should intercept it at a value of ΔP equal to $\sigma^2\pi^0$. The intercept was normally larger than this and he postulated that an intermediate compartment in the root was responsible for the shift. Since then, we have used the term effective external osmotic pressure (π^0_e) to designate the actual extrapolated intercept (5, 6, 10). As a mathematical convenience we will now use the term π^* to indicate the difference between the actual π^0 and π^0_e (Fig. 1B). More will be said about π^* later but it is sufficient to note here that use of this term allows us to rewrite the volume flux equation as

$$J_v = L_p[\Delta P - \sigma(\pi^0 - \pi^i) - \pi^*], \quad (4)$$

where L_p is the hydraulic conductance coefficient in m^3 m^{-2} s^{-1} MPa^{-1}, ΔP is the hydrostatic pressure difference between the outside of the root and the xylem and π^* characterizes the effect of the intermediate compartment. Upon accounting for the volume flux dependence of π^i we get

$$J_v = L_p\left[\Delta P - \sigma\pi^0 - \pi^* + \frac{\sigma\pi^0(1 - \sigma)J_v + \sigma RT(\omega\pi^0 + J_s^*)}{J_v + \omega RT}\right]. \quad (5)$$

Consideration of Equation 5 shows that the extrapolated intercept is now $\sigma^2\pi^0 + \pi^*$, which will satisfy Newman's test.

Rearrangement of Equation 5 now gives us the quadratic form of the volume flux:

$$J_v^2 + J_v[\omega RT - L_p(\Delta P - 2\sigma\pi^0 + \sigma^2\pi^0 - \pi^*)] - L_pRT(\omega\Delta P + \sigma J_s^* - \omega\pi^*) = 0, \quad (6)$$

which is very similar to previously published equations (4, 5, 10). Neither this model nor any of the previous ones take any account of possible exclusively apoplastic flows (15) which would appear as convective solute flows.

Equations 2 and 6 are the functions to which the data were fitted to obtain the transport coefficients L_p, σ, J_s^*, ω, and π^* in an attempt to see which ones varied in such a way as to account for the marked diurnal changes in volume flux under conditions of constant ΔP. Figure 1, A and B, which are the averages of the data for each pressure over the 24-h period, will be used to illustrate the curve fitting procedure.

CURVE FITTING

The solute and volume flux data were fitted to Equations 2 and 6, respectively, using the nonlinear least squares program 'NLLSQ' by CET Research Group, Ltd., Norman, OK.[1]

The first step of the procedure was to fit the $J_s - J_v$ data to Equation 2 to obtain a value for σ. Because the slope of the line at high J_v is dominated by σ (Fig. 1A and Eq. 3), no weighting of the data was necessary to obtain a good fit. Using the value of σ thus obtained, we then fitted the data to Equation 6 to obtain the additional parameters L_p, J_s^*, ω, and π^*. In this instance, however, it was necessary to weight the data for low values of J_v in order to estimate ω and J_s^* in the portion of the $J_v - \Delta P$ curve where they most influence J_v.

RESULTS AND DISCUSSION

Table I contains the values of the various transport coefficients determined from the 24-h solute and volume flux averages. The solid curves in Figure 1, A and B, are the theoretical solute and volume fluxes calculated from Equations 2 and 6 using these 24-h averages. The line shown in Figure 1A is calculated from the final parameters determined from the $J_v - \Delta P$ fit and not the original $J_s - J_v$ fit which was used only to determine σ.

The r^2 values (0.9921 for Fig. 1B and 0.8674 for Fig. 1A) indicate that the overall fit is acceptable for both curves but obviously much better for the $J_v - \Delta P$ data. The greatest uncer-

Table I. *Volume and Solute Transport Coefficients for Data Averaged over 24-h Period*

Coefficient	Value	Standard Error	Units	SE/$\bar{X}$
σ	0.9822	0.0108		0.011
J_s^*	3.784×10^{-8}	1.209×10^{-8}	mole m^{-2} s^{-1}	0.320
ω	5.253×10^{-7}	1.941×10^{-7}	mole m^{-2} s^{-1} MPa^{-1}	0.369
π^*	0.0564	0.0054	MPa	0.096
L_p	2.983×10^{-7}	0.0872×10^{-7}	m s^{-1} MPa^{-1}	0.029

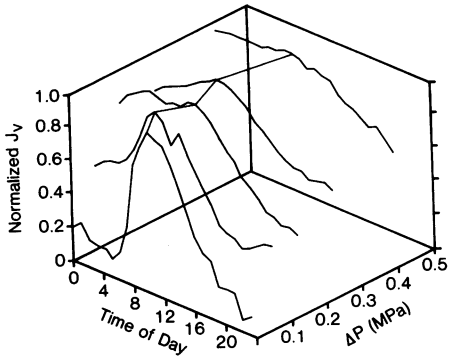

FIG. 2. Diurnal volume flux for 5 of the 10 root systems. Each curve was normalized to the maximum observed J_v for that system. Each system was held at a constant pressure for the duration of the experiment. Only 5 of the 10 curves are shown to reduce clutter in the figure. The line across the top connects the points of maximum J_v.

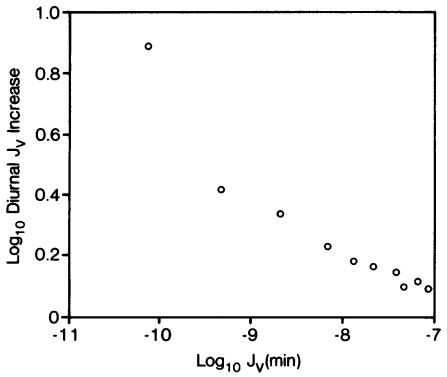

FIG. 3. Relationship between the fractional diurnal peak and the minimum J_v for all 10 plants, showing the inverse relationship between peak size and J_v. Fractional peak size is calculated as $(J_v^{max} - J_v^{min})/J_v^{min}$.

tainty is in the values for J_s^* and ω (Table I) which show SE/$\bar{X} \cong$ 30 to 40%, whereas the coefficient of variability for the other parameters is only 1 to 10%. This is true for each of the hourly values as well as the 24-h averages.

The diurnal course of the normalized volume flux is shown in Figure 2 for 5 of the 10 steady state pressures. The results for the other 5 pressures are not shown to reduce clutter. The data in Figure 2 were normalized to the maximum observed diurnal J_v at each pressure so that the diurnal changes could be compared even though there were two orders of magnitude difference in J_v between the highest and lowest ΔP values. The most obvious fact emerging from these data is that the relative diurnal change, with peak fluxes around 1000 h, was quite large at low ΔP and decreased as the pressure difference, and consequently J_v, increased. Note also, for later reference, that there was a tendency for J_v to decline during the experimental period. This decline was most obvious at higher flows suggesting a regular decline in L_p. It should also be mentioned here that although specific tests were not conducted during this experiment, unpublished data from numerous (50–100) other experiments indicate that the

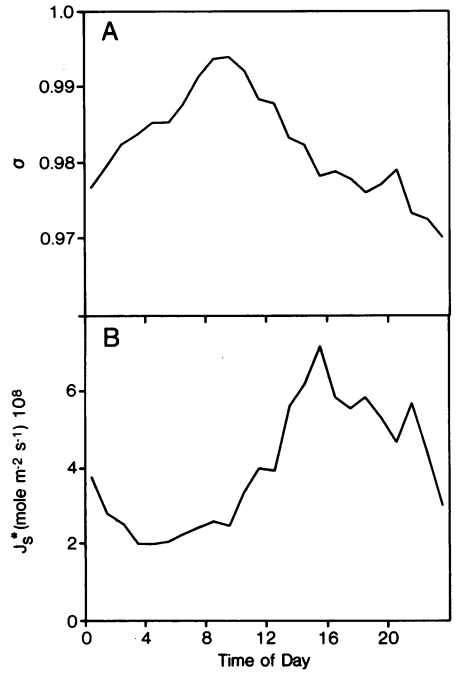

FIG. 4. Diurnal values for the reflection coefficient (σ) and the active component of nutrient transport (J_s^*).

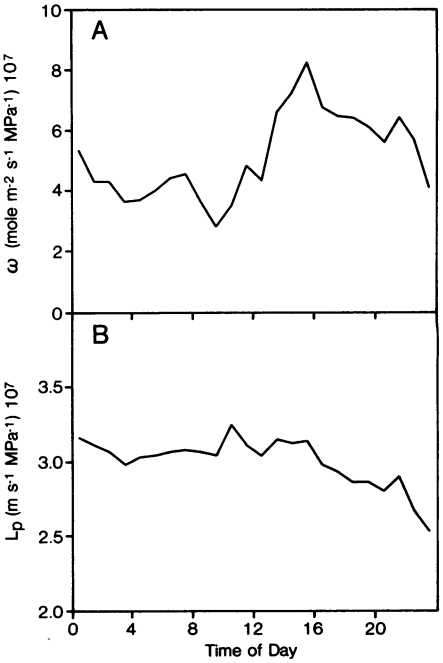

FIG. 5. Diurnal values for the coefficient of solute mobility (ω) and the hydraulic conductance coefficient (L_p).

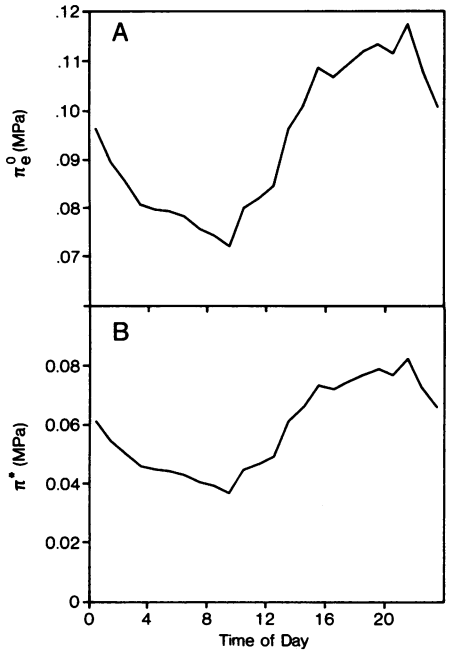

FIG. 6. Diurnal values for the effective external osmotic pressure (π_e^0) and π^*. Note that $\pi_e^0 = \pi^* +$ a constant π^0 (= 35 kPa).

diurnal peak occurs around midday regardless of when the plants are decapitated.

The relationship between the relative size of the diurnal peak and the minimum J_v for each ΔP is shown in Figure 3, which includes all 10 data points. Within reason, then, we can say from observing Figure 3 that the degree of diurnal change in root conductance is inversely related to the existing value of J_v. This observation is important since it indicates that any diurnal rhythm in L_p is certainly not the cause of the rhythm in volume flux. If L_p were the major cause, then we would see the relative size of the diurnal peaks increase with volume flux rather than decrease. That Figure 3 is not a mathematical artifact due to having the same variable on both axes is confirmed by a very similar relationship when the relative diurnal peak is plotted as a function of ΔP.

Figures 4 to 6 show how each of the transport parameters varied through the 24-h period. There are substantial changes in all the parameters except L_p, which shows an overall decline during this time. Superimposed on this overall pattern of decline may be a relatively small diurnal rhythmic variation on the order of 10%, with a maximum between 1000 and 1500 h.

While σ reached its maximum value at about 1000 h, J_s^*, π^*, and ω all achieved their maxima later in the day. Note that π^* is negatively correlated with J_v, with its lowest values occurring at about 1000 when J_v achieves its diurnal peak.

We can now use the estimates of the temporally varying transport parameters to simulate the diurnal rhythms in volume and solute fluxes. To accomplish this and for no other reason than to keep the result as neat as possible, we rotated the diurnal parameters (Figs. 4–6) so that the beginning and ending values were the same. The rotation was accomplished by joining the beginning and ending points with a straight line. All the data values were then adjusted up or down to keep the same relationship with that line when it was rotated to a horizontal position. The desired result was to cancel out the effects of the systematic deterioration of the root system evident in Figures 2 and 4 to 6. This procedure was adopted for aesthetic reasons only and will not change any of the following arguments or conclusions.

The resulting simulations appear in Figure 7. The calculated volume fluxes as a function of ΔP (Fig. 7A) conform well to the

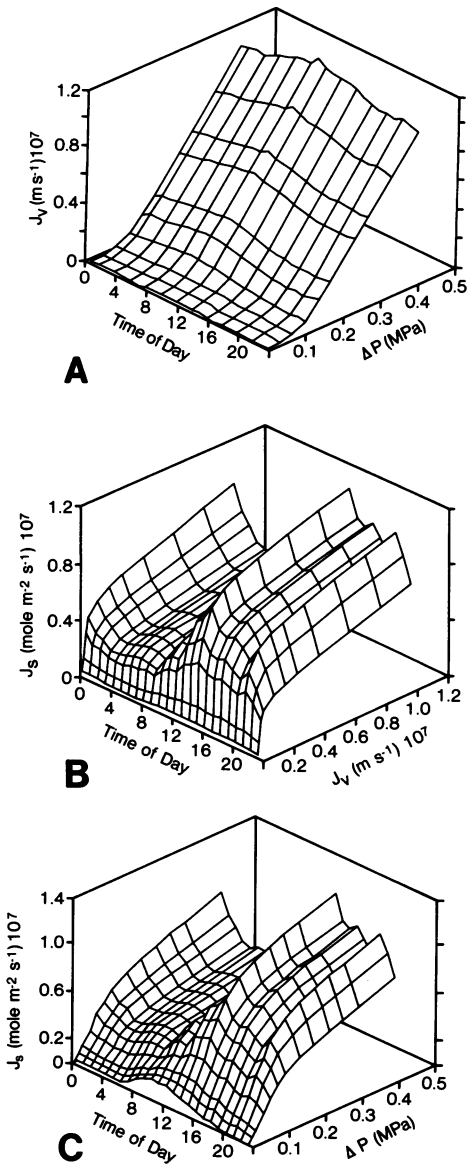

FIG. 7. Simulations of volume and solute fluxes. Lines for each hour were calculated from Equations 2 and 6 and the rotated values of the coefficients given in Figures 4 to 6.

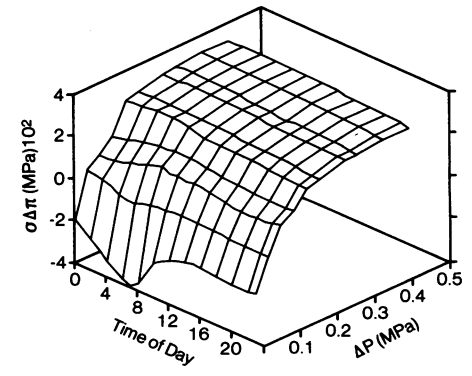

FIG. 8. The measured effective osmotic pressure difference between the root medium and the xylem exudate. A negative value for $\sigma\Delta\pi$ means a net force directed toward the xylem.

data with an average r^2 for the 24 separate fits of 0.989 ± 0.005. Solute fluxes as a function of J_v fit much less well as judged by an average r^2 of 0.629 ± 0.128. Reexamination of Figure 1A reveals that the scatter of the $J_s - J_v$ data, even for the 24 h averages, is much larger than for the $J_v - \Delta P$ plot. Obviously, the 24 individual curves had even greater scatter.

The solute fluxes are plotted through time as functions of J_v (Fig. 7B) and ΔP (Fig. 7C). These figures show that the mode of plotting can influence the interpretation of the diurnal changes in volume flux. Note that when J_s is plotted against J_v (Fig. 7B) there is an obvious peak of J_s at about 1500 h and that this peak appears at the same time of day regardless of J_v. However, when J_s is plotted across lines of equal ΔP the appearance of the peak shifts from 1000 to 1200 h at low ΔP, which corresponds to the peak in J_v, to about 1500 h at higher levels of applied pressure. At higher pressures and consequently higher volume fluxes, the diurnal rhythms in J_s seen in Figure 7, B and C, are very similar.

The prime motivation for the preceding exercise is that it is very difficult experimentally to obtain data across lines of equal volume flux. Figure 7C, therefore, represents the most likely type of plot resulting directly from experimental data, but Figure 7B represents the functional relationship between J_s and J_v needed to fit the data. The level of applied pressure then would have a great deal to do with the time when the peak in J_s would be observed.

Interpreting volume fluxes in terms of ion transport thus becomes a difficult problem. This becomes even more evident when the relationship between ΔP and the osmotic pressure difference across the root is considered (Fig. 8). The measured $\Delta\pi$ between the xylem exudate and the external solution was multiplied by the estimated σ for each hour. The result shows that there is a very definite diurnal peak in the osmotic pressure difference, especially at low ΔP values. However, this peak is not correlated with the volume flux peak and, in fact, occurs at about 0700, several h prior to the J_v peak (Fig. 2).

An important conclusion from Figures 7, B and C, and 8 is that it is extremely difficult to draw conclusions regarding the causes of flux changes from such data. There are two major problems involved. First, there is no way at present to account for either standing gradient effects (1) or for reabsorption of solutes from the xylem (17). Both of these processes will have a similar effect in making the exudate more dilute when it exits the root system than it was at the main site of osmotically induced volume flux, presumably deep within the root. Second, it is very difficult to account for the time lag involved in moving the solution from the depths of the root, at the site of action, to the cut stump, where the measurements are made. In this regard there is an additional complication: if there is a change in the volume flux during the time the solution is resident in the root then the solution may be either diluted or concentrated as a result of that change in J_v. In short, it is difficult, if not impossible, to draw worthwhile conclusions from the root exudate except when the flow rates are high so that the standing gradient effects and the resident times are minimized. Even with the analysis we have used in this paper, there is greater uncertainty for transport coefficients whose estimates rely most heavily on data obtained at low J_v (*viz.* ω and J_s^*).

Because of the difficulties mentioned above of relating the rhythm in volume flux to rhythms in the transport coefficients or total solute fluxes, further analysis is required to interpret the effects of the changes in the coefficients. The interplay between the different parameters would be difficult to envision even if they didn't change. Since all the parameters do change, and not all in phase with each other, the interpretational task is compounded. Therefore, as an aid to understanding the complex relationships involved, we will consider the total differential of the volume flux at constant π^0 and ΔP.

$$dJ_v = \left(\frac{\partial J_v}{\partial \sigma}\right)_{\omega,J_s^*,\pi^*,L_p} d\sigma + \left(\frac{\partial J_v}{\partial \omega}\right)_{\sigma,J_s^*,\pi^*,L_p} d\omega + \left(\frac{\partial J_v}{\partial J_s^*}\right)_{\sigma,\omega,\pi^*,L_p} dJ_s^* + \left(\frac{\partial J_v}{\partial \pi^*}\right)_{\sigma,\omega,J_s^*,L_p} d\pi^* + \left(\frac{\partial J_v}{\partial L_p}\right)_{\sigma,\omega,J_s^*,\pi^*} dL_p = \sum C_{x_i} dx_i. \quad (7)$$

Evaluation of each of the partial differential coefficients in Equation 7 is straightforward but messy and will be left to the appendix. We may, however gain some insight into the operation of the system if we examine the interplay between the diurnal changes in both the partial differential coefficients and the related transport parameters.

The interplay of the five transport parameters is difficult to envision because not only do they all vary diurnally but so do the partial differential coefficients. To assign importance, or lack thereof, to any of the parameters, we calculated the percentage of the diurnal change that could be attributed to each of the parameters over the range of ΔP from 0 to 0.5 MPa. The calculations were performed as follows. The values of each of the transport parameters were noted for the times of the daily min and daily max J_v, for each of the 10 steady state pressures. Each of the partial differential coefficients was evaluated for the time of minimum J_v. From the observed finite change in the parameter (between the time of min and max J_v) and the value of its partial differential coefficient, the expected finite change in J_v due to the change in that particular parameter was calculated as the product $C_{x_i}\,\Delta x_i$. The ΔJ_v calculated for each parameter was then expressed as a percentage of the total change in J_v caused by the combined action of all five parameters. Figure 9 shows the relative contributions of each of the five parameters over the pressure range.

One of the first things to note is that the contribution of each parameter can be strongly dependent on the applied pressure and therefore the volume flux. Also, the contributions of the various parameters may seem to run counter to intuition. For example, although C_{J_s}* always has positive values, the effect of the changes in J_s* are observed to be negative (Fig. 9). This is because at the time between the minimum and the diurnal peak, the value of J_s* actually declined (see Figs. 2 and 4B), so that its contribution to J_v was negative.

As can be seen, above applied pressures of about 0.2 MPa only L_p and π* are important determinants of J_v. At lower applied pressures and resulting J_v, the solute transport parameters σ, ω, and J_s* become much more important as has been shown in other contexts in the past (4–6, 8–10). The only parameter that is important across the entire range of ΔP is π*. A point worth reiterating about the influence of these parameters is that each should be considered within the context of the size of the diurnal peak relative to the baseline fluxes. Although we see that the influence of L_p increases to account for 70% of the diurnal peak at 0.5 MPa, the diurnal peak at that pressure is only about 17% over the baseline.

Figure 9 then illustrates the complexity of the processes which cause the diurnal changes in volume flux in *Phaseolus* root systems. At low fluxes, ω, J_s*, and π* dominate the process and at high fluxes only L_p and π* are important in producing the diurnal changes. Note again that Figure 9 is only for the average values of the transport parameters for the 24-h period and that these relationships can be expected to change diurnally. We feel, however, that little would be accomplished by presenting further details at this time.

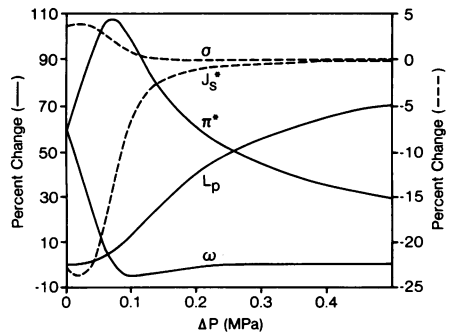

FIG. 9. The fractional contribution of each of the 5 transport coefficients to the diurnal peak of volume flux. Dashed lines refer to the right hand ordinate. At any pressure all the contributions sum to 100%. An even better perspective may be obtained by comparing with Figures 2 and 3.

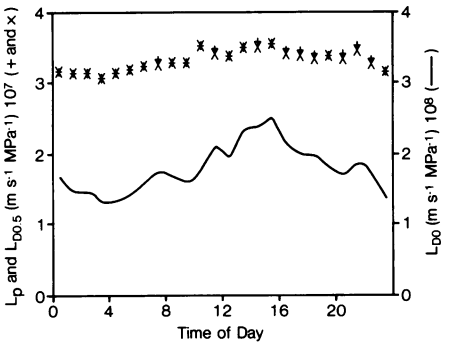

FIG. 10. Comparison of L_p with L_D at 2 different applied pressures, 0 MPa (L_{D0}) and 0.5 MPa ($L_{D0.5}$) showing the convergence of L_D with L_p at higher applied pressures and therefore higher flow rates. The means of $L_{D0.5}$ and L_p are about 20 times the mean for L_{D0}.

In addition to our interest in discovering the causes of the diurnal rhythms in volume flux through the roots, we also would like to know a little about how the various parametric rhythms might affect the water balance of the whole plant. In this regard we will restrict our considerations to the conductance to volume flux that the root system presents to the shoot and the way that the conductance varies diurnally and with the xylem tension. We showed in an earlier paper that the xylem tension could be replaced by the ΔP that we have been using in this analysis so that a differential conductance (9) of the root system may be formed which is, for all other parameters constant,

$$L_D = \frac{dJ_v}{d\Delta P} = \frac{L_p}{2} + \frac{L_p}{2}\left[\frac{f_1(\Delta P)}{f_2(\Delta P)}\right]. \quad (8)$$

The full expression is given in the appendix. It is sufficient to note here that over the ΔP range of 0 to 0.5 MPa, the L_D based on the diurnal averages for the transport parameters went from about 4% to 99% of L_p, about a 20-fold change. This behavior is possible because the ratio of the functions f_1 and f_2 in Equation 8 ranges from negative values at low ΔP, through 0, and approaches 1 as ΔP gets large. L_D, therefore, approaches L_p at higher ΔP values. Figure 10 illustrates the extremes of this relationship over the range of pressures used in this paper. An important point to note in this figure is that the peak in L_D for $\Delta P = \phi(L_{D\phi})$ does not coincide with the peak in J_v (Fig. 2) and is, in fact, 5 h out of phase with it. This situation may run counter to the intuition of some readers but consideration of the definition of L_D (Eq. 8) shows that it is, in fact, undefined for conditions where ΔP is constant.

The use of L_D as defined in Equation 8 needs some explanation since ΔP is only a part of the total driving force across the root system. The differential conductance with respect to ΔP was chosen because we were trying to arrive at a mathematical description of the root system which was consistent with its operation in the intact plant. Therefore, since water is normally driven through the roots by the tension in the xylem (ΔP) this particular conductance was chosen as the most logical one to use in this context. It should also be noted that even though we are considering a conductance with respect to ΔP, the osmotic component of the driving force is not being ignored. It is functionally located, in a somewhat complicated form, in Equations 8 and 17 which allow its dependence on the xylem tension to be expressed. Thus, from the viewpoint of the whole plant, water flow through the roots is normally driven by the pressure potential in the xylem and the variable osmotic component of the force is a complicated function of that pressure potential.

Under the circumstances an accurate description of the system may be obtained by writing J_v as a function of time ($J_v = J_v[t]$). This may be done, of course, by replacing each of the transport parameters in Equation 6 with its own temporal function (determined by fitting the curves in Figs. 4–6). In essence, that is how the simulations of J_v, J_s, and L_D were accomplished. The difference was that for those simulations we used the discrete estimates of the parameters, from which Figures 4 to 6 were constructed, and not mathematically defined temporal functions.

Because of the temporally fluctuating nature of the various transport parameters there appears to be no single coefficient, such as the instantaneous conductance (9) or resistance, that can be calculated to describe the root system through time. Although it is quite possible to divide the solution of Equation 6 by ΔP to obtain an instantaneous conductance, there seems little reason to do so since we would already possess the information necessary to describe the system. On the other hand, it clearly would be very difficult to reverse the procedure and infer anything very useful about the various parameters simply by measuring ΔP and the flux and calculating an instantaneous conductance or resistance, even when the parameters are constant. In cases like this, temporal functions are both more realistic and more useful.

If we wish, we may now also impose on the system of temporally fluctuating coefficients, $\Delta P = \Delta P(t)$. The purpose in doing so would be to simulate the effects of diurnal changes in transpiration driven water flow through the plant.

The transport equations used here and in the past (4–6, 8–10) to describe volume and solute fluxes through root systems are operational in nature and not meant to reflect a detailed anatomical or physiological knowledge of the root system. These equations describe quite adequately for present purposes, how the root system acts when subjected to pressure differences meant to mimic the naturally occurring tension in the xylem. Although these equations resemble those meant to describe solute and volume fluxes through single isotropic membranes (16), only brief consideration is necessary to conclude that the resemblence is superficial. All the coefficients are defined operationally and each one is the result of interaction between a complex series/parallel arrangement of cells and cell membranes each with its own system of volume and solute transport coefficients. For example, σ is defined operationally as the result of some property(-ies) of the system which allows only a fraction of those solutes carried to the root surface by virtue of being dissolved in the water to pass through the root and appear in the exudate. One can easily imagine that fraction to represent entirely apoplastic flows made possible by small breaks or leaks in the root system or to leakiness of some bounding membrane(s). One can also imagine, with equal validity, that the same effect could be produced by solution passing through channels between cells which extract solutes from the solution as it passes. In a previous

paper (5) we derived the following expression from Equation 3:

$$C^i = \frac{J_s}{J_v} \cong C^0(1 - \sigma) + (\omega\pi^0 + J_s^*)\left(\frac{1}{J_v}\right), \quad (9)$$

which gives C^i as a linear function of J_v^{-1} with intercept C^0 $(1 - \sigma)$. This intercept provided the basis of the operational definition of σ as

$$\sigma = 1 - \left(\frac{C^i}{C^0}\right) J_v \to \infty. \quad (10)$$

In short, σ is defined only in terms of what is on the outside and what appears in the exudate regardless of the means of exclusion or removal of the solutes during passage.

Incidentally, the 24-h average σ determined graphically from Equation 10 agrees with the value determined from the nonlinear curve fitting routine used in this paper to within less than 0.5%.

Another case in point is π^*. We easily can observe its effects but details about its causes are difficult to obtain. We have been able to show in the past (6, 8) that there is some type of osmotically active compartment in the root which opposes inwardly directed volume flux. It appears that this compartment contains normally nonmobile solutes which are asymmetrically distributed. Treatment with a growth regulator (ABA) allowed these solutes to move into the xylem and simultaneously removed the effect of π^* (6, 8). Little more detail is currently available about π^* except that the observations of Wallace *et al.* (28) and Hanson and Biddulph (14) are consistent with the diurnal shifts in π^* which we observed. They observed more uptake of radioactive tracers during the night and more translocation to the shoot during the day. Thus uptake and sequestering of nutrients during the late afternoon and night might increase π^* and slow down J_v. Then during the day when conditions for translocation to the shoot are more favorable due to increased transpiration these nutrients might be released to the xylem thus reducing π^* and allowing increased volume flux through the root system.

Also, it seems possible that π_e^0 is closely related to, if not the same as, the intercept (p_0) of the transpiration-balance pressure curves of Passioura and Munns (22). They observed increases of p_0 from morning to afternoon and speculated that this shift in p_0 might have been responsible for the diurnal cycling in root resistance observed by Parsons and Kramer (21). Such speculation is certainly consistent with our interpretation of the effects of π^*, which was also observed to increase from morning to afternoon (Fig. 6). So, given the assessment of the importance of π^* in determining the diurnal transport rhythms, more detailed information about the causes and location of π^* would contribute greatly to our basic understanding of root system function.

All the other coefficients are similarly operationally defined and not meant to correspond to the properties of any particular single membrane but to describe the operation of the entire tissue, which they appear to do reasonably well.

In this paper we have drawn one step closer to understanding diurnal changes in water and solute transport. The question of mechanisms, however, still remains unanswered. We have shown how each of the transport coefficients changes diurnally but we cannot say what makes them change. Perhaps they are influenced by rhythms in root growth or carbohydrate or growth regulator transport to the roots as some workers have suggested (3, 14, 25, 26). Until we understand more about the fundamental mechanisms or structures which manifest themselves as these coefficients, we will probably not discover why they change the way they do.

LITERATURE CITED

1. ANDERSON WP, DP AIKMAN, A MEIRI 1970 Excised root exudation—a standing gradient osmotic flow. Proc Roy Soc B174: 459–468
2. BARRS HD, B KLEPPER 1968 Cyclic variations in plant properties under constant environmental conditions. Physiol Plant 21: 711–730
3. BUNCE JA 1978 Effects of shoot environment on apparent root resistance to water flow in whole soybean and cotton plants. J Exp Bot 29: 595–601
4. FISCUS EL 1975 The interaction between osmotic- and pressure-induced water flow in plant roots. Plant Physiol 55: 917–922
5. Fiscus EL 1977 Determination of hydraulic and osmotic properties of soybean root system. Plant Physiol 59: 1013–1020
6. FISCUS EL 1981 Effects of abscisic acid on the hydraulic conductance of and the total ion transport through *Phaseolus* root systems. Plant Physiol 68: 169–174
7. FISCUS EL 1981 Analysis of the components of area growth of bean root systems. Crop Sci 21: 909–913
8. FISCUS EL 1982 Effects of abscisic acid in the root: communication between the shoot and root. *In* PF Wareing, ed, Plant Growth Substances 1982. Academic Press, New York, pp 591–598
9. FISCUS EL 1983 Water transport and balance within the plant: resistance to water flow in roots, *In* HM Taylor, WR Jordan, TR Sinclair, eds, Limitations to Efficient Water Use in Crop Production. American Society of Agronomy, Madison, WI, pp 183–194
10. FISCUS EL, A KLUTE, MR KAUFMANN 1983 An interpretation of some whole plant water transport phenomena. Plant Physiol 71: 810–817
11. GROSSENBACHER KA 1938 Diurnal fluctuation in root pressure. Plant Physiol 13: 669–676
12. GROSSENBACHER KA 1939 Autonomic cycle of rate of exudation in plants. Am J Bot 26: 107–109
13. HAGAN RM 1949 Autonomic diurnal cycles in the water relations of nonexuding detopped root systems. Plant Physiol 24: 441–454
14. HANSON JB, O BIDDULPH 1953 The diurnal variation in the translocation of minerals across bean roots. Plant Physiol 28: 356–370
15. HANSON PJ, EI SUCOFF, AH MARKHART III 1985 Quantifying apoplastic flux through red pine root systems using trisodium, 3-hydroxy-5,8,10-pyrenesulfonate. Plant Physiol 77: 21–24
16. KATCHALSKY A, PF CURRAN 1965 Nonequilibrium Thermodynamics in Biophysics. Harvard University Press, Cambridge, MA
17. KLEPPER B 1967 Effects of osmotic pressure on exudation from corn roots. Aust J Biol Sci 20: 723–735
18. MACDOWELL FDH 1964 Reversible effects of chemical treatments on the rhythmic exudation of sap by tobacco roots. Can J Bot 42: 115–122
19. NEWMAN EI 1966 A method of estimating the total length of root in a sample. J Appl Ecol 3: 139–145
20. NEWMAN EI 1976 Interaction between osmotic and pressure induced water flow in plant roots. Plant Physiol 57: 738–739
21. PARSONS LR, PJ KRAMER 1974 Diurnal cycling in root resistance to water movement. Physiol Plant 30: 19–23
22. PASSIOURA JB, R MUNNS 1984 Hydraulic resistance of plants. II. Effects of rooting medium, and time of day, in barley and lupin. Aust J Physiol 11: 341–350
23. SKIDMORE EL, JF STONE 1964 Physiological role in regulating transpiration rate of the cotton plant. Agron J 56: 405–410
24. SKOOG F, TC BROYER, KA GROSSENBACHER 1938 Effects of auxin on rates, periodicity, and osmotic relations in exudation. Am J Bot 25: 749–759
25. TRUBETSKOVA OM, IL SHIDLOVSKAYA 1951 Study of the daily periodicity of activity of the root system. Fiziol Rast 7: 273–290
26. TRUBETSKOVA OM, NG ZHIRNOVA 1959 Diurnal rhythm of potassium transfer from the root system to the aerial organs of plants. Fiziol Rast 6: 129–137
27. VAADIA Y 1960 Autonomic diurnal fluctuations in rate of exudation and root pressure of decapitated sunflower plants. Physiol Plant 13: 701–717
28. WALLACE A, SM SOUFI, N HEMAIDAN 1966 Day-night differences in the accumulation and translocation of ions by tobacco plants. Plant Physiol 41: 102–104
29. WHITE PR 1942 "Vegetable Dynamicks" and plant tissue culture. Plant Physiol 17: 153–164

APPENDIX

Starting from Equation 6, we may simplify matters by letting

$$a = 1$$

$$b = \omega RT - L_p(\Delta P - 2\sigma\pi^0 + \sigma^2\pi^0 - \pi^*),$$

$$c = -L_p RT(\omega\Delta P + \sigma J_s^* - \omega\pi^*),$$

$$d = b^2 - 4ac,$$

$$g = \omega\Delta P + \sigma J_s^* - \omega\pi^*, \text{ and}$$

$$h = \Delta P - 2\sigma\pi^0 + \sigma^2\pi^0 - \pi^*.$$

The solution of Equation 6 for J_v is from the standard quadratic

formula:

$$J_v = \frac{-b + \sqrt{d}}{2}. \tag{11}$$

The partial differential coefficients are simply formed as the appropriate first derivative of Equation 11 with all the other coefficients held constant.

$$\left(\frac{\partial J_v}{\partial \sigma}\right)_{\omega,J_s^*,\pi^*,L_p} = L_p\left[\frac{RTJ_s^* + b\pi^0(1-\sigma)}{\sqrt{d}} - \pi^0(1-\sigma)\right] \tag{12}$$

$$\left(\frac{\partial J_v}{\partial \omega}\right)_{\sigma,J_s^*,\pi^*,L_p} = \frac{RT}{2}\left[\frac{2L_p(\Delta P - \pi^*) + b}{\sqrt{d}} - 1\right] \tag{13}$$

$$\left(\frac{\partial J_v}{\partial J_s^*}\right)_{\sigma,\omega,\pi^*,L_p} = \frac{\sigma L_p RT}{\sqrt{d}} \tag{14}$$

$$\left(\frac{\partial J_v}{\partial \pi^*}\right)_{\sigma,\omega,J_s^*,L_p} = -\frac{L_p}{2}\left[\frac{RT\omega + L_p h}{\sqrt{d}} + 1\right] \tag{15}$$

$$\left(\frac{\partial J_v}{\partial L_p}\right)_{\sigma,\omega,J_s^*,\pi^*} = \frac{h}{2} + \frac{2RTg - bh}{2\sqrt{d}}. \tag{16}$$

Likewise, the full expression for L_D (Eq. 8) is

$$L_D = \frac{dJ_v}{d\Delta P} = \frac{L_p}{2} + \frac{L_p}{2}\left[\frac{2\omega RT - h}{\sqrt{d}}\right]. \tag{17}$$